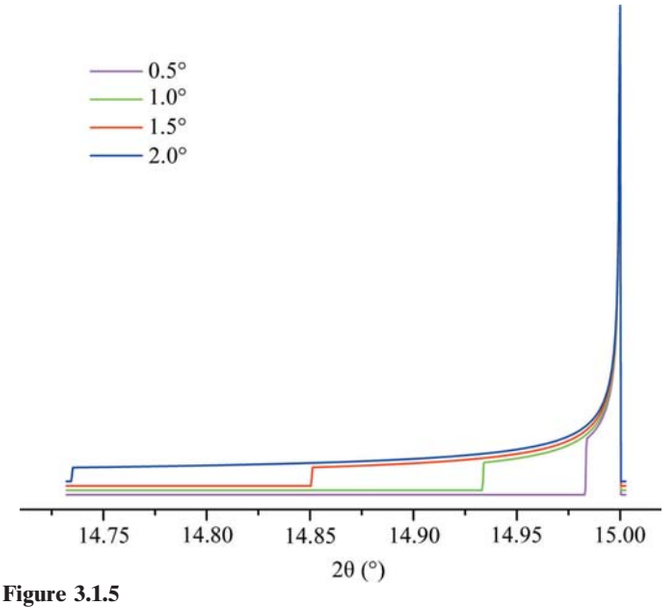

Figure 3.1.5
The flat specimen error aberration profile as a function of incident-slit size (R = 217.5 mm).

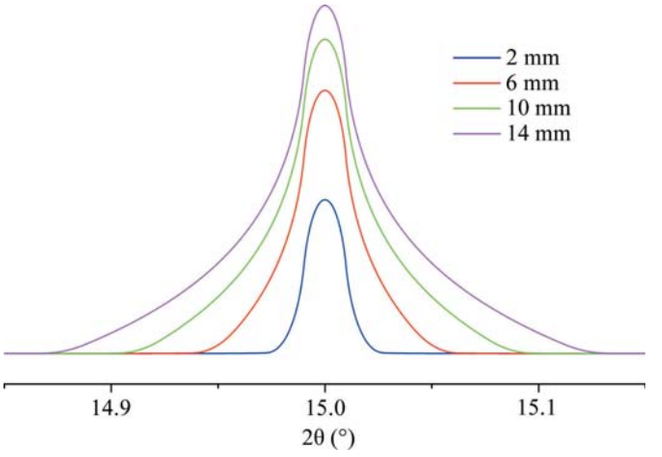

Figure 3.1.7
The PSD defocusing error aberration profiles for a silicon strip PSD as a function of window width (R = 217.5 mm, incident slit = 1° and strip width = 75 μm).

proportional to the divergent slit size as shown in Fig. 3.1.5. Its functional dependence on 2θ angle, *i.e.* 1/tan θ, is illustrated in Fig. 3.1.6. The flat specimen error leads to asymmetric profile broadening on the low-angle side, accentuated at decreasing values of 2θ. The functional dependence of this aberration on 2θ, shown in Fig. 3.1.6, is for a fixed slit; the use of a variable-divergence incident-beam slit to obtain a constant area of illumination reduces this dependence on the 2θ angle.

The broadening imparted to diffraction line profiles from the early gas-flow proportional PSDs was due to defocusing originating from both the equatorial width of the PSD window and parallax within the gas-filled counting chamber. Early models for these effects (Cheary & Coelho, 1994) included two parameters: one for the window width and a second for the parallax. The modern silicon strip PSDs do not need this second term as there is effectively no parallax effect. The aberration profile imparted to the data from a modern PSD (Mendenhall *et al.*, 2015) is illustrated in Fig. 3.1.7 as a function of window width. The profiles are symmetric about the centre line, exhibiting both increasing intensity and breadth as the window width is increased. The profile consists of two components: a central peak with a width independent of 2θ, which is due to the pixel strip width of the detector, and wings which are due to the defocusing. The breadths of the wings shown in Fig. 3.1.7 vary in proportion to the incident slit size and as 1/tan θ, and therefore are largely unobservable at high 2θ angles.

Cheary & Coelho (1998*a*,*b*) have modelled axial divergence effects in the context of two geometric cases. Case 1 is the situation in which the axial divergence is limited solely by the width of the beam path as determined by the length of the tube filament, the receiving slit and the size of the sample. The aberration function in which these parameters are 12 mm, 15 mm and 15 mm, respectively, is illustrated in Fig. 3.1.8; the extent of broadening is nearly 1° in 2θ at a 2θ angle of 15°. The other plots of Fig. 3.1.8 refer to a 'case 2' situation where axial divergence is limited by the inclusion of Soller slits in the incident- and diffracted-beam paths. One also has to consider the impact of a including a graphite post-monochromator. This would increase

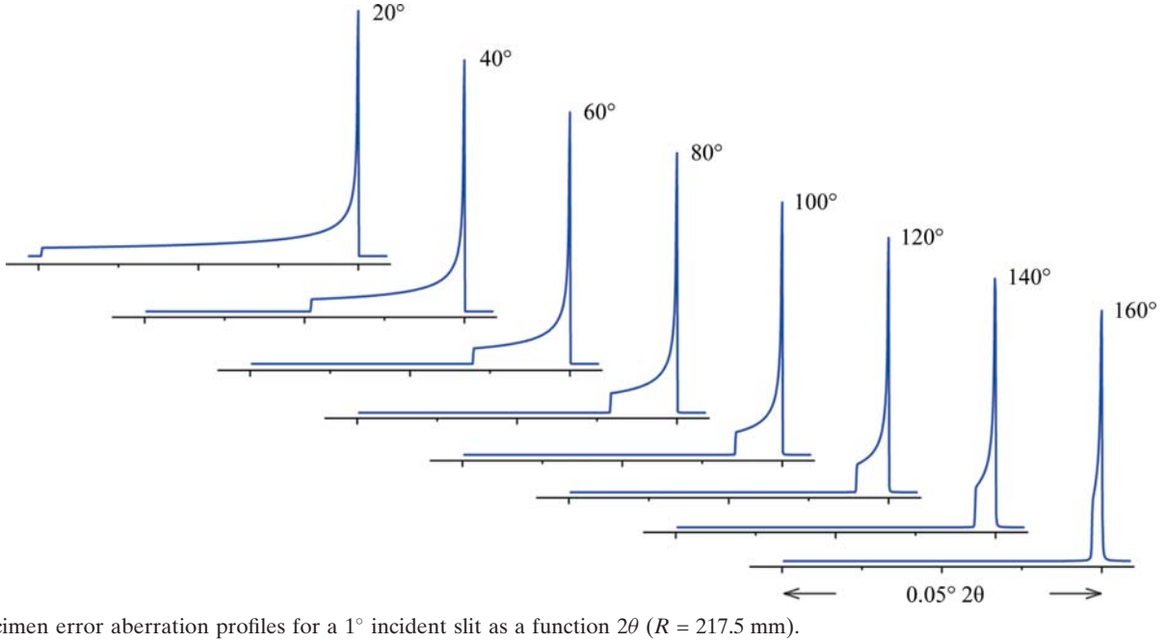

Figure 3.1.6
The flat specimen error aberration profiles for a 1° incident slit as a function 2θ (R = 217.5 mm).